ELECTRICAL ENGINEERING

T 190

ELEKTROS INŽINERIJA

Equations of DC Corona Electric Wind Velocities

P. Marčiulionis, S. Žebrauskas

Department of Theoretical Electrical Engineering, Kaunas University of Technology,
Studentų str. 48, LT-51367 Kaunas, Lithuania, phone: +370 37 300268; e-mail: stasys.zebrauskas@ktu.lt

Introduction

The phenomenon of electric corona discharge in air occurs due to ionising collisions of electrons with neutral gas molecules in the strong electric field near the electrode with small radius of surface curvature and is associated with a transport of ions to an electrode with opposite sign of potential. Most applications of corona discharge (electrostatic precipitation, electrophotography, ionization instrumentation, control of acid gases from combustion sources, generation of ozone, etc.) are related to this charge transport in the outer zone of the discharge [1]. The movement of ions from the discharge electrode to the other electrode is obstructed by collisions with electrically neutral air molecules, and it is a reason to rise the electrohydrodynamic flow known as the electric or ionic wind. This phenomenon causes the application of corona discharge in electrohydrodynamic pumps, in electric micromachines, in inkjet systems, is used for enhancement of the heat and mass exchange processes [2,3]. There are many papers representing the results of experimental [4] and theoretical investigations [1,3,5]. Because of the complexity of the problem theoretical investigation involves numerical methods, such as finite difference , finite element or boundary element method. Most of these papers deal with research of electric wind in the pin-to-plate electrode system. This paper is devoted to the numerical investigation of electric wind in wire-to-plate electrode system by using the finite difference method.

Equations of electric wind velocities

Incompressible and viscous airflow induced by Coulomb force $\boldsymbol{F} = \rho \cdot \boldsymbol{E} = \boldsymbol{J}/b$ (ρ – the density of ionic charge, $\boldsymbol{E}$ – electric field strength of the discharge, $\boldsymbol{J}$ – corona current density, and b – ion mobility assumed as constant) is determined by the system of equations comprising of the Navier-Stokes equation and the equation of flow continuity (for steady-state conditions) [1]:

$$\begin{cases} (\boldsymbol{v} \cdot \nabla)\boldsymbol{v} = \dfrac{\boldsymbol{F}}{\rho_a} - \dfrac{\nabla p}{\rho_a} + \nu\Delta\boldsymbol{v}, \\ \nabla \cdot \boldsymbol{v} = 0, \end{cases} \quad (1)$$

where $\boldsymbol{v}$ is the air velocity, p is the pressure, ρ_a is the density of air, and ν is the kinematic viscosity of air ($\rho_a = 1{,}15$ kg/m^3 = const., and $\nu = 1{,}58 \times 10^{-5}$ m/s^2 = const. under assumption). Many authors [4] use the Cartesian system of coordinates for generation of computational grid and for solving the system of equations (1). We choose the polar system of coordinates for the electric and the airflow field can be assumed as the plane one [2]. Boundary conditions on the surface of the wire can be formulated simply if the centre of the wire is coincided with the origin of the coordinate system and the regular grid of the polar coordinate system is used (Fig. 1). Equations (1) can be transformed to the following form for the components v_r and v_φ of the air flow velocity (in polar system of coordinates r, φ) [6]:

$$\frac{v_r\partial v_r}{\partial r} + \frac{v_\varphi\partial v_r}{r\partial\varphi} - \frac{v_\varphi^2}{r} = \frac{F_r}{\rho_a} - \frac{\partial p}{\rho_a\partial r} + \nu\left[\Delta v_r - \frac{2\partial v_\varphi}{r^2\partial\varphi} - \frac{v_r}{r^2}\right], \quad (2)$$

$$\frac{v_r\partial v_\varphi}{\partial r} + \frac{v_\varphi\partial v_\varphi}{r\partial\varphi} + \frac{v_r v_\varphi}{r} = \frac{F_\varphi}{\rho_a} - \frac{\partial p}{\rho_a r\partial\varphi} +$$
$$+ \nu\left[\Delta v_\varphi + \frac{2\partial v_r}{r^2\partial\varphi} - \frac{v_\varphi}{r^2}\right], \quad (3)$$

$$\frac{\partial v_r}{\partial r} + \frac{1}{r}\frac{\partial v_\varphi}{\partial\varphi} = 0, \quad (4)$$

where

$$\Delta v_r = \frac{1}{r}\frac{\partial}{\partial r}\left(r\frac{\partial v_r}{\partial r}\right) + \frac{1}{r^2}\frac{\partial^2 v_r}{\partial\varphi^2}, \quad (5)$$

and

$$\Delta v_\varphi = \frac{1}{r}\frac{\partial}{\partial r}\left(r\frac{\partial v_\varphi}{\partial r}\right) + \frac{1}{r^2}\frac{\partial^2 v_\varphi}{\partial\varphi^2}. \quad (6)$$

The field of electrohydrodynamic airflow velocities can be assumed as free jet flow with constant air pressure [7]. Therefore the derivatives $\partial p/\partial r$ and $\partial p/\partial\varphi$ are equal to 0 in all areas except the vicinity of a plane electrode.

Finite approximation of equations for irregular grid

First derivatives of equations (2), (3) and (4) can be found by using the central differences [8]:

$$\begin{cases} \dfrac{\partial v_r}{\partial r} = \dfrac{v_{rQ} - v_{rS}}{a_Q + a_S}, & \dfrac{\partial v_\varphi}{\partial r} = \dfrac{v_{\varphi Q} - v_{\varphi S}}{a_Q + a_S}, \\[2mm] \dfrac{\partial v_r}{\partial \varphi} = \dfrac{v_{rR} - v_{rP}}{a_R + a_P}, & \dfrac{\partial v_\varphi}{\partial \varphi} = \dfrac{v_{\varphi R} - v_{\varphi P}}{a_R + a_P}, \\[2mm] \dfrac{\partial p}{\partial r} = \dfrac{p_Q - p_S}{a_R + a_P}, & \dfrac{\partial p}{\partial \varphi} = \dfrac{p_R - p_P}{a_R + a_P}. \end{cases} \quad (7)$$

Finite difference approximation of Laplacian for irregular grid in polar coordinate system:

$$\Delta v_r = \frac{v_{rP}}{a_P(a_P + a_R)} + \frac{v_{rR}}{a_R(a_P + a_R)} + \frac{v_{rQ}(2r + a_S)}{2ra_Q(a_Q + a_S)} +$$

$$+ \frac{v_{rS}(2r - a_Q)}{2ra_S(a_Q + a_S)} - v_{rO}\left(\frac{1}{a_P a_R} + \frac{2r + a_S - a_Q}{2ra_Q a_S}\right), \quad (8)$$

$$\Delta v_\varphi = \frac{v_{\varphi P}}{a_P(a_P + a_R)} + \frac{v_{\varphi R}}{a_R(a_P + a_R)} + \frac{v_{\varphi Q}(2r + a_S)}{2ra_Q(a_Q + a_S)} +$$

$$+ \frac{v_{\varphi S}(2r - a_Q)}{2ra_S(a_Q + a_S)} - v_{\varphi O}\left(\frac{1}{a_P a_R} + \frac{2r + a_S - a_Q}{2ra_Q a_S}\right). \quad (9)$$

The distances a_Q, a_S, a_R and a_P from the neighbour nodes to the central node O of a computational grid are shown in Fig. 1.

Substituting formulas (7), (8) and (9) into equations (2)–(4) yields the main equations of computation for irregular grid in polar coordinate system. Difference approximation of the equation (2) is the following:

$$v_{rO}\frac{v_{rQ} - v_{rS}}{a_Q + a_S} + \frac{v_{\varphi O}}{r}\left(\frac{v_{rR} - v_{rP}}{a_R + a_P}\right) - \frac{v_{\varphi O}^2}{r} = \frac{F_{rO}}{\rho_a} +$$

$$+ \nu\Big[\frac{v_{rP}}{a_P(a_P + a_R)} + \frac{v_{rR}}{a_R(a_P + a_R)} + \frac{v_{rQ}(2r + a_S)}{2ra_Q(a_Q + a_S)} - \frac{v_{rO}}{r^2} +$$

$$+ \frac{v_{rS}(2r - a_Q)}{2ra_S(a_Q + a_S)} - \frac{v_{rO}}{a_P a_R} - \frac{v_{rO}(2r + a_S - a_Q)}{2ra_Q a_S} +$$

$$+ \frac{2}{r^2}\left(\frac{v_{\varphi R} - v_{\varphi P}}{a_R + a_P}\right)\Big] - \frac{1}{\rho_a}\left(\frac{p_Q - p_S}{a_R + a_P}\right), \quad (10)$$

difference approximation of the equation (3):

$$v_{rO}\frac{v_{\varphi Q} - v_{\varphi S}}{a_Q + a_S} + \frac{v_{\varphi O}}{r}\left(\frac{v_{\varphi R} - v_{\varphi P}}{a_R + a_P}\right) + \frac{v_{rO}v_{\varphi O}}{r} = \frac{F_{\varphi O}}{\rho_a} +$$

$$+ \nu\Big[\frac{v_{\varphi P}}{a_P(a_P + a_R)} + \frac{v_{\varphi R}}{a_R(a_P + a_R)} + \frac{v_{\varphi Q}(2r + a_S)}{2ra_Q(a_Q + a_S)} - \frac{v_{\varphi O}}{r^2} +$$

$$+ \frac{v_{\varphi S}(2r - a_Q)}{2ra_S(a_Q + a_S)} - \frac{v_{\varphi O}}{a_P a_R} - \frac{v_{\varphi O}(2r + a_S - a_Q)}{2ra_Q a_S} +$$

$$+ \frac{2}{r^2}\left(\frac{v_{rR} - v_{rP}}{a_R + a_P}\right)\Big] - \frac{1}{\rho_a r}\left(\frac{p_R - p_P}{a_R + a_P}\right), \quad (11)$$

and the approximation of the equation (4):

$$\frac{v_{rQ} - v_{rS}}{a_Q + a_S} + \frac{1}{r}\frac{v_{\varphi R} - v_{\varphi P}}{a_R + a_P} = 0. \quad (12)$$
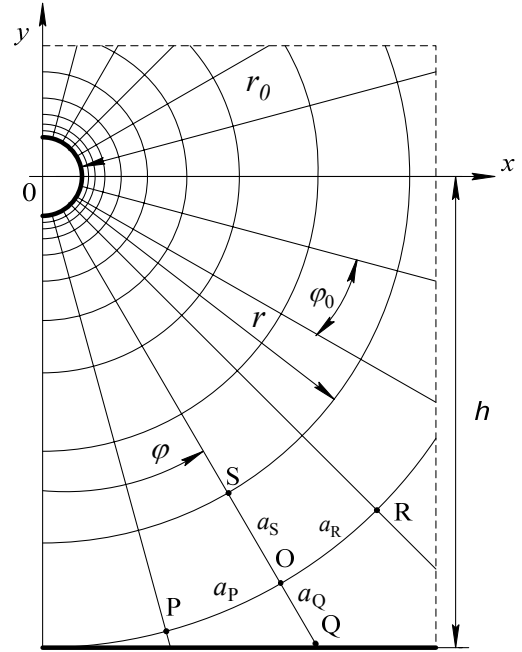

Fig. 1. Computational grid in polar coordinate system

Computational equations for a regular grid

Equations (10)–(12) are used for areas near plane electrode and near open straight boundaries of the field. These equations can be simplified for use in the areas with a regular grid. The determining parameter of a regular grid is the grid size m related with an elementary central angle φ_0 (Fig. 1) by an equation:

$$\varphi_0 = \frac{\pi}{m}. \quad (13)$$

The radial coordinate r is a power function of a number i of the node in a row:

$$r = r_0\beta^{i-1}, \quad (14)$$

where $\beta = 1 + \varphi_0$.

Substituting (14) into (10)–(12) gives

$$v_{rO}\frac{v_{rQ} - v_{rS}}{r_0\beta^i\left(1 - 1/\beta^2\right)} + v_{\varphi O}\frac{v_{rR} - v_{rP}}{2\varphi_0\left(r_0\beta^{i-1}\right)^2} -$$

$$- \frac{v_{\varphi O}^2}{r_0\beta^{i-1}} = \frac{F_{rO}}{\rho_a} - \frac{p_Q - p_S}{2\rho_a\varphi_0 r_0\beta^{i-1}} +$$

$$+ \nu\left[\Delta v_r - \frac{v_{rO}}{\left(r_0\beta^{i-1}\right)^2} - 2\frac{v_{\varphi R} - v_{\varphi P}}{2\varphi_0\left(r_0\beta^{i-1}\right)^3}\right], \quad (15)$$

$$v_{rO}\frac{v_{\varphi Q} - v_{\varphi S}}{r_0\beta^i\left(1 - 1/\beta^2\right)} + v_{\varphi O}\frac{v_{\varphi R} - v_{\varphi P}}{2\varphi_0\left(r_0\beta^{i-1}\right)^2} +$$

$$+ \frac{v_{rO}v_{\varphi O}}{r_0 \beta^{i-1}} = \frac{F_{\varphi O}}{\rho_a} - \frac{p_R - p_P}{2\rho_a \varphi_0 (r_0 \beta^{i-1})^2} +$$

$$+ \nu \left[\Delta v_\varphi - \frac{v_{\varphi O}}{(r_0 \beta^{i-1})^2} + 2 \frac{v_{rR} - v_{rP}}{2\varphi_0 (r_0 \beta^{i-1})^3} \right], \quad (16)$$

$$\frac{v_{rQ} - v_{rS}}{r_0 \beta^i (1 - 1/\beta^2)} + \frac{v_{\varphi R} - v_{\varphi P}}{2\varphi_0 (r_0 \beta^{i-1})^2} = 0. \quad (17)$$

Discrete formula of Laplacian is invariant to coordinate r:

$$\Delta v_r = v_{rP} + v_{rR} + \frac{2 + 3\varphi_0}{2 + \varphi_0} v_{rQ} + \frac{(2 - \varphi_0)(1 + \varphi_0)^2}{2 + \varphi_0} v_{rS} -$$

$$- \frac{8(1 + \varphi_0) - \varphi_0^3}{2 + \varphi_0} v_{rO}, \quad (18)$$

$$\Delta v_\varphi = v_{\varphi P} + v_{\varphi R} + \frac{2 + 3\varphi_0}{2 + \varphi_0} v_{\varphi Q} + \frac{(2 - \varphi_0)(1 + \varphi_0)^2}{2 + \varphi_0} v_{\varphi S} -$$

$$- \frac{8(1 + \varphi_0) - \varphi_0^3}{2 + \varphi_0} v_{\varphi O}. \quad (19)$$

Coulomb force

Many authors [1,3,5] use the numerical method of Coulomb force F computation based upon a solving the system of corona field equations [9]. We present there the results of analytical computation of the force F obtained by the use of Deutsch-Popkov assumption [7]:

$$\boldsymbol{E}_2 = \vartheta \boldsymbol{E}_1, \quad (20)$$

where $\boldsymbol{E}_1$ is the electrostatic field strength, $\boldsymbol{E}_2$ is the corona field strength, and ϑ is the scalar function of coordinates. Modulus of the force $\boldsymbol{F}$ and components F_x, F_y for Cartesian coordinate system are determined in [2]. The values of x and y in the formulas of E_{2x} and E_{2y} presented in [2] can be found for given r and φ (Fig. 2):

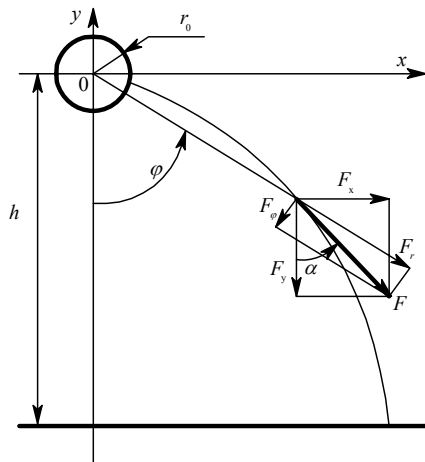$$x = r\sin\varphi, \quad y = h - r\cos\varphi. \quad (21)$$

Fig. 2. The components of the Coulomb force $\boldsymbol{F}$

The angle α (Fig. 2) depends upon F_x and F_y:

$$\alpha = \arctan(F_x / F_y). \quad (22)$$

The components F_r and F_φ are the function of $\varphi - \alpha$:

$$F_r = F \cos(\varphi - \alpha), \quad (23)$$

$$F_r = F \cos(\varphi - \alpha). \quad (24)$$

$F_\varphi = 0$ and $F_r = F$ for points of symmetry axis ($x = 0$).

The distribution of electrostatic field strength E_1, corona field strength E_2, charge density ρ and the force F on the axis of symmetry for $r_0 = 0,005$ mm, $h = 12$ mm, $U = 10$ kV and constant ion mobility equal to 2,20 cm²/Vs is given in the Table 1.

Table 1. Distribution of electrostatic field strength E_1, corona field strength E_2, charge density ρ and force F on the symmetry axis

y, mm	E_1, MV/m	E_2, MV/m	ρ, µC/m³	F, N/m³
−0,05	32,476	15,841	3216,4	50951,6
−1	1,690	1,206	2663,0	3211,3
−2	0,883	0,783	1949,1	1525,4
−3	0,617	0,704	1469,3	1034,1
−4	0,486	0,686	1170,5	802,8
−5	0,409	0,688	974,9	670,5
−6	0,360	0,702	836,3	586,7
−7	0,327	0,722	734,8	530,6
−8	0,304	0,748	658,3	492,1
−9	0,288	0,779	598,0	465,8
−10	0,278	0,816	549,9	448,6
−11	0,272	0,859	510,9	438,9
−12	0,270	0,910	478,7	435,8

The distribution of the force F on the surface of plane electrode is shown in Fig. 3. Variation of the value of force on this surface is from 430 N/m³ in the centre to 120 N/m³ in peripheral points. Variation of force on the axis of symmetry is more considerable: from 50950 N/m³ on the surface of the wire to 430 N/m³ on the surface of plate (see the table), the ratio of these values is 118. Moreover, considerable variation of the force is in the area near the surface of the wire.
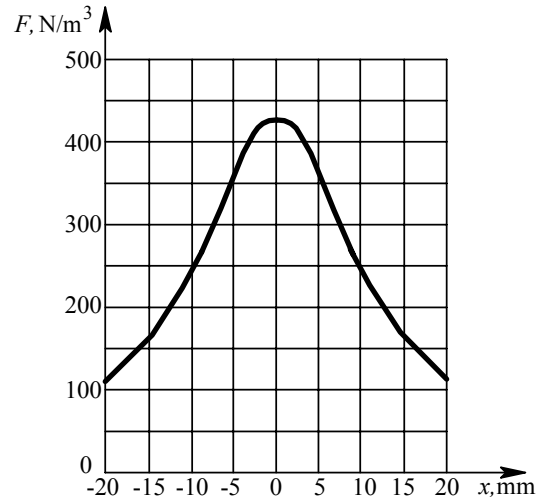

Fig. 3. Distribution of the force F on the surface of plate

Small size of the regular polar grid in this area corresponds to the zone of intense variation of the force. On the other hand, irregular grid is used in the area near the surface of the plane electrode. The variation of the force isn't so remarkable in this area therefore the size of the grid is considerable at the surface of plane electrode. The distances a_Q, a_S, a_R and a_P (Fig. 1) can be calculated by using the elementary geometrical relationships. If the Cartesian coordinate system is used the problem can't be solved without multiple reducing the size of computational grid near the surface of the wire.

Conclusions

1. Difference approximation of equations describing the electric wind velocities in wire-to-plane electrode system is presented for irregular and regular grids.
2. Polar coordinate system is used because of remarkable variation of Coulomb force in the area near the surface of the wire.

References

1. **Zhao L., Adamiak K.** EHD Flow in Air Produced by Electric Corona Discharge in Pin-Plate Configuration // Journal of Electrostatics. – 2005. – Vol. 63, No. 3-4. – P. 337 – 350.
2. **Žebrauskas S., Ramanauskas A.** Vienpolio vainikinio išlydžio elektrinio vėjo greičių skaičiavimas// Elektronika ir elektrotechnika. – 2002. – Nr. 5(54). – P. 70 – 75.
3. **Kawamoto H., Yasuda H., Umezu S.** Flow Distribution and Pressure of Air due to Ionic Wind in Pin-to-Plate Corona Discharge System // Journal of Electrostatics. – 2006. – Vol. 64, No. 6. – P. 400 – 407.
4. **Rickard M., Dunn-Rankin D., Weinberg F., Carleton F.** Maximizing Ion-Driven Gas Flows // Journal of Electrostatics. – 2006. – Vol. 64, No. 6. – P. 368 – 376.
5. **Lastow O., Balachandran W.** Numerical Simulation of Electrohydrodynamic Atomization // Journal of Electrostatics. – 2006. – Vol. 64, No. 12. – P. 850 – 859.
6. **Kundu P. K., Cohen I. M.** Fluid Mechanics, 2nd Ed. – 2002. – 766 p.
7. **Верещагин И. П.** Высоковольтные электротехнологии. – Изд. МЭИ, 1999. – 199 p.
8. **Chung T. J.** Computational Fluid Dynamics. – Cambridge University Press Pb, 2002. – 1022 p.
9. **Žebrauskas S., Marčiulionis P.** Elektrodų sistemos „laidas šalia cilindro" vienpolio vainikinio išlydžio elektrinis laukas // Elektronika ir elektrotechnika. – 2006. – Nr. 1(65). – P. 43 – 47.

P. Marčiulionis, S. Žebrauskas. Equations of DC Corona Electric Wind Velocities // Electronics and Electrical Engineering. – Kaunas: Technologija, 2007. – No. 8(80). – P. 73–76.

Electrohydrodynamic movement of air is a phenomenon associated with corona discharge. It is widely used in modern technologies. Equations of electric wind in electrode systems with wire corona electrodes are discussed. Difference approximation of the Navier-Stokes equation and the equation of continuity for plane air flow is presented for irregular and regular grids in polar coordinate system. The Coulomb force initiating electric wind is computed analytically using the Deutsch-Popkov assumption. The variation of the force on the axis of symmetry is more significant in comparison with that on the surface of plane electrode. It is the reason of using the polar coordinate system because the grid is regular and of small size in the area near the surface of the wire where the variation of the force is mostly considerable and the values of the force are the greatest. Ill.3, bibl. 9 (in English; summaries in Lithuanian, English and Russian).

П. Марчюленис, С. Жебраускас. Уравнения скоростей электрического ветра униполярного коронного разряда // Электроника и электротехника. – Каунас: Технология, 2007. – № 8(80). – С. 73–76.

Явление электрогидродинамического движения воздуха связано с коронным разрядом. Оно широко используется в современных технологиях. Обсуждены уравнения электрического ветра для систем с проволочными коронирующими электродами. Приведены выражения разностной аппроксимации уравнений Навье-Стокса и непрерывности плоского потока для нерегулярной и регулярной сеток в полярной системе координат. Определяющая движение воздуха кулоновская сила определена аналитически в результате расчета поля короны на основе допущения Дойча-Попкова. Изменение силы на оси симметрии поля в несколько порядков превышает изменение на поверхности плоского электрода. Это является причиной выбора полярной системы координат, так как в области у поверхности провода с быстрым изменением силы регулярная сетка довольно мелкая. Ил. 3, библ. 9 (на английском языке; рефераты на литовском, английском и русском яз.).

P. Marčiulionis, S. Žebrauskas. Vienpolio vainikinio išlydžio elektrinio vėjo greičių lygtys // Elektronika ir elektrotechnika. – Kaunas: Technologija, 2007. – Nr. 8(80). – P. 73–76.

Elektrinis vėjas yra vienas iš vainikinio išlydžio pašalinių reiškinių, plačiai taikomas šiuolaikinėse technologijose. Aptartos elektrodų sistemų su vieliniais elektrodais vainikinio išlydžio elektrinio vėjo lygtys. Pateikta Navier ir Stokeso, taip pat plokščiojo tekėjimo srauto tolydumo lygčių skirtuminė aproksimacija polinės koordinačių sistemos netaisyklingam ir taisyklingam tinkleliams. Elektrinį vėją lemianti Kulono jėga apskaičiuota analitiškai remiantis Deutscho ir Popkovo prielaida. Lauko simetrijos ašyje ši jėga keičiasi daug labiau negu plokščiojo elektrodo paviršiuje. Dėl šios priežasties pasirinkta polinė koordinačių sistema, kadangi lauko srityje prie vainikinio išlydžio elektrodo paviršiaus, kur jėga kinta sparčiausiai ir kur jos vertės yra didžiausios, taisyklingo polinio tinklelio žingsnis yra gana smulkus. Il. 3, bibl. 9 (anglų kalba; santraukos lietuvių, anglų ir rusų k.).